International Journal of Automotive Technology, Vol. 19, No. 4, pp. 651−658 (2018)
DOI 10.1007/s12239−018−0062−8

pISSN 1229−9138/ eISSN 1976−3832

REAL-TIME LONGITUDINAL LOCATION ESTIMATION OF VEHICLE CENTER OF GRAVITY

Jounghee Lee[1)*], Dongyoon Hyun[1)], Kyoungseok Han[2)] and Seibum Choi[2)]

[1)] Research & Development Division, Hyundai Motor Company, 150 Hyundaiyeonguso-ro, Namyang-eup, Hwaseong-si, Gyeonggi 18280, Korea
[2)]School of Mechanical, Aerospace & System Engineering, KAIST, Daejeon 34141, Korea

(Received 28 July 2017; Revised 10 November 2017; Accepted 20 December 2017)

ABSTRACT−The longitudinal location of a vehicle's center of gravity (CG) is used as an important parameter for vehicle safety control systems, and can change considerably according to various driving conditions. Accordingly, for the better performance of vehicle safety control systems, it is essential to obtain the accurate CG location. However, it is generally difficult to acquire the value of this parameter directly through sensors due to cost reasons. In this study, a practical algorithm for estimating vehicle's longitudinal CG location in real time is proposed. This algorithm is derived based only on longitudinal motion of the vehicle, excluding excessive lateral, yaw and roll movements of the vehicle. Moreover, the proposed algorithm has main differences from previous studies in that it does not require information such as vehicle mass, vehicle moments of inertia, road grade or tire-road surface friction, which are difficult to acquire. In the proposed algorithm, the relationship between the ratio of rear-to-front tire longitudinal force and the corresponding wheel slips are used to determine the CG location. To demonstrate a practical use of the proposed algorithm, the ideal brake force distribution is tested. The proposed CG estimation algorithm and its practical use are verified via simulations and experiments using a test vehicle equipped with electro-mechanical brakes in the rear wheels. It is shown that the estimated CG locations are close to the actual ones, and that the deceleration can be maximized by the ideal brake force distribution.

KEY WORDS : Center of Gravity (CG), Parameter estimation, Adaptive observer, Brake force distribution

1. INTRODUCTION

Due to cost reasons, some of the vehicle parameters used for vehicle safety control are not readily measurable or cannot be calibrated through sensors in real-time. In these cases, these parameters can be treated as constant. Likewise, the longitudinal location of a vehicle's center of gravity (CG) is often assumed constant as in many papers related to vehicle safety control (Choi, 2008; Han *et al*., 2017, Kim *et al*., 2001; Yoon *et al*., 2006). However, the CG location can change considerably depending on various driving conditions, compared to the parameters such as the wheelbase and the track width that hardly change. For example, the number of passengers, amount of luggage and their corresponding position can affect the variation of CG location. This variation is not negligible, especially for light weight vehicles, since the CG location may change significantly (Huang and Wang, 2014).

The longitudinal location of a vehicle's center of gravity (CG) is used as an essential parameter in various chassis control systems. For example, this CG location plays an important role in determining the individual vertical tire forces. Subsequently, these vertical tire forces are utilized to acquire the tire-road friction information for the anti-lock brake systems (ABS) and traction control systems (TCS) (Ulsoy *et al*., 2012). In addition, these tire forces are utilized to optimally distribute the traction/braking forces on the front and rear wheels so that vehicle's acceleration/deceleration can be maximized (Peng and Hu, 1996). Furthermore, the longitudinal CG location is utilized as one of the main parameters in determining the desired vehicle yaw rate or side-slip angle in electronic stability control systems (ESC) (Rajamani, 2006). By using the estimated CG location instead of the fixed location which can be significantly different from the actual CG location, precise information of individual vertical tire forces can be obtained. Therefore, the estimation of the longitudinal CG location plays a critical role in improving the performance of chassis control systems such as ABS, TCS, ESC, etc.

Several different approaches have been proposed for estimating the longitudinal CG location. Most of these studies utilized the persistent yaw or roll motion (Solmaz *et al*., 2008; Wenzel *et al*., 2006; Wesemeier and Isermann, 2009), which may cause a loss of stability, in order to acquire accurate estimation results. To avoid the excitations in the directions of lateral/yaw/roll, some other studies have proposed using the longitudinal-motion-based estimator (Huang and Wang, 2012, 2014). In these studies,

**Corresponding author.* e-mail: jhmail@hyundai.com

the additional parameters and states, such as the vehicle mass, road slope or tire-road friction, are required for CG location estimation. Furthermore, to identify the information of additional parameters, a special vehicle equipped with in-wheel motors (or axle motors) at front and rear wheels was utilized. However, these parameters and states are known to be difficult to acquire in production vehicles (Pence *et al*., 2014; Rajamani *et al*., 2012).

An important distinction between the method presented in this paper and other conventional methods is that proposed real-time estimation algorithm does not require information such as vehicle mass, vehicle moments of inertia, road grade or tire-road surface friction, which are difficult to acquire. To minimize required information of additional parameters for the estimation algorithm, a new strategy was adopted, that utilizes the ratio of rear-to-front tire longitudinal force and corresponding wheel slips. The wheel slips are obtained using GPS and wheel speed sensors. Since both front and rear longitudinal tire forces are not zero during braking, the estimation algorithm is derived based on the longitudinal dynamic model during braking. In addition, this algorithm only uses the longitudinal motion of the vehicle, excluding the excessive lateral, yaw and roll movements of the vehicle. Furthermore, an adaptive law is adopted to reduce the effects of sensor noises and road roughness, thus enabling the real-time estimation of the longitudinal CG location.

To demonstrate a practical use of the proposed algorithm, the estimated CG location was utilized for ideally distributing braking force among the vehicle's wheels, which can provide the maximum deceleration before the wheels become locked. The proposed CG estimation algorithm was verified through simulations and experiments using a test vehicle equipped with electro-mechanical brakes(EMB) in the rear wheels.

2. LONGITUDINAL VEHICLE MODEL

The vehicle model used for this study is related to equations for the vertical/longitudinal forces on the tires and the rotational dynamics of the wheels.

2.1. Vertical Forces on the Tires

The forces acting on a vehicle moving on a slope are depicted in Figure 1. The vertical tire forces on the axles can be derived by the moment balance as follows:

$$F_{zf} = (L_r / L - (\dot{V}_x / g + \sin(\theta_{road})) \cdot h / L) \cdot mg \quad (1)$$

$$F_{zr} = (L_f / L + (\dot{V}_x / g + \sin(\theta_{road})) \cdot h / L) \cdot mg \quad (2)$$

where *f*, *r* mean front and rear, respectively.

The information about the longitudinal acceleration and the road grade can be achieved from the longitudinal acceleration sensor measurements as follows:

$$a_{x,sens} = \dot{V}_x + g\sin(\theta_{road} + \theta_{pitch}) \quad (3)$$

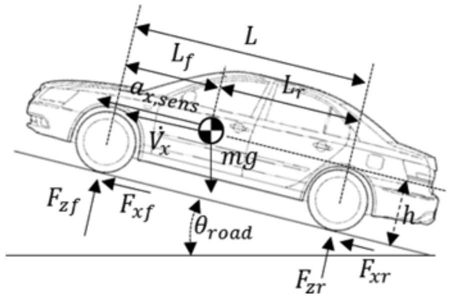

m	: Vehicle mass
L	: Wheelbase
L_f	: Distance of the CG from the front axle
L_r	: Distance of the CG from the rear axle
h	: CG height
$a_{x,sens}$	: Longitudinal Acceleration from sensor
$\dot{V}_x$	: Longitudinal Acceleration of the vehicle
θ_{road}	: Road Grade

Figure 1. Vehicle model on a slope.

where θ_{pitch} is the pitch angle of the vehicle.

Since the pitch angle is typically small under normal braking conditions compared to the sum of the vehicle longitudinal acceleration and the road grade effect, it is neglected for simplicity.

Consequently, defining the normalized CG location as $\chi = L_f/L$, Equations (1) and (2) can be expressed in terms of χ and $a_{x,sens}$ as follows:

$$F_{zf} = (1 - \chi + a_{x,g} \cdot h / L) \cdot mg \quad (4)$$

$$F_{zr} = (\chi - a_{x,g} \cdot h / L) \cdot mg \quad (5)$$

where $a_{x,g} = -a_{x,sens}/g$ is the longitudinal deceleration measurements in g-units.

Equations (4) and (5) show that the CG location can be determined without road grade information if individual tire vertical forces and vehicle mass can be identified. However, it is difficult to identify individual tire vertical forces and vehicle mass without additional sensors. Thus, to estimate the CG location without additional sensors, a new method is proposed, using the fact that the vertical tire forces on both axles are proportional to the vehicle mass. Details will be discussed in Section 3.

2.2. Longitudinal Forces on the Tires

Longitudinal tire forces can be derived from the rotational dynamics of the wheels as follows:

$$J_{w,i}\dot{\omega}_i = (T_{d,i} - T_{b,i}) - R \cdot F_{x,i} \quad (6)$$

where the subscript i = *fl*, *fr*, *rl*, *rr* represents the four wheels of the vehicle. $T_{d,i}$, $T_{b,i}$ represent the drive torque and brake torque. R and $F_{x,i}$ are the tire effective radius and the longitudinal tire forces, respectively. The drive torque can be calculated from the engine torque available over the CAN bus of the vehicle. The brake torque is described as follows:

$$T_{b,i} = \mu_{pad,i} \cdot F_{cl,i} \cdot r_{eff,i} \tag{7}$$

where $\mu_{pad,i}$, $F_{cl,i}$, $r_{eff,i}$ are the brake pad friction coefficient, clamping force acting on the brake pad and the effective radius of brake, respectively.

Consequently, the longitudinal tire force can be expressed by Equations (6) and (7) as follows:

$$F_{x,i} = (T_{d,i} - \mu_{pad,i} \cdot F_{cl,i} \cdot r_{eff,i} - J_{w,i} \cdot \dot{\omega}_i) / R \tag{8}$$

Based on Equation (8), the longitudinal tire forces can be determined using the drive torque from CAN, brake clamping force from brake control unit and wheel speed from sensor signals.

3. CG LOCATION ESTIMATION

The aforementioned equations of vertical tire forces and longitudinal tire forces can be integrated by the linear relationship between the normalized tire force and corresponding wheel slip ratio in the low slip region. However, the normalized tire force varies as the tire-road friction changes, and it is a nontrivial task to estimate the CG location without information about the tire-road friction. Furthermore, the vehicle mass has to be known to calculate the vertical tire forces. For this reason, a new strategy based on the rear-to-front tire longitudinal force ratio is suggested, and a basic equation about the longitudinal CG location is presented, which does not require information about the vehicle mass or tire-road friction. To compensate the uncertainties of the basic equation caused by sensor noises and road roughness, an adaptive scheme is applied.

3.1. Tire Model

Figure 2 describes the well-known relationship between the normalized tire force and the tire slip-ratio (Han *et al.*, 2017; Khalil and Grizzle, 1996). When the vehicle is braking in a straight line, the front and rear wheel slips are generated by the corresponding longitudinal forces and the tire vertical forces which are depicted as P1 and P2 in Figure 2, respectively. In mild braking conditions, the front wheel slip is normally greater than the rear one, and there are some gaps between the front and rear wheel slips for safety reasons. As the braking force increases, the gap between P1 and P2 becomes narrower, and they approach together to P3 due to the electronic brake force distribution (EBD) control.

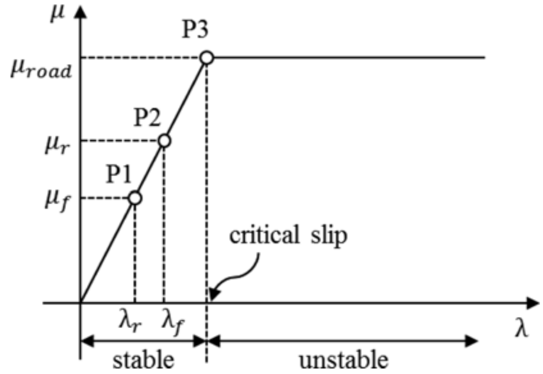

Figure 2. Mu-slip curve.

The normalized tire force during braking is defined as follows:

$$\mu_i = -F_{x,i} / F_{z,i} \tag{9}$$

where the subscript $F_{z,i}$ is the vertical load of each tire. The slip ratio during braking is defined as follows:

$$\lambda_i = (V_x - R \cdot \omega_i) / V_x \tag{10}$$

where V_x, ω_i are the longitudinal velocity of the vehicle and the wheel rotational speed, respectively.

In the low slip region, depicted as stable in Figure 2, the normalized tire force is proportional to the slip ratio for any given road surface. Since most braking conditions arise within the stable region, the normalized tire force can be expressed through multiplying the proportion, *i.e.* slip slope, and slip ratio as follows:

$$\mu_i = C_{x,i} \cdot \lambda_i \tag{11}$$

where $C_{x,i}$ is defined as the slip slope of each tire.

Considering that a vehicle usually uses the same tire on all wheels and that the vehicle is moving on a homogeneous road surface in most of the actual driving conditions, the slip slope can be assumed as common value, C_x, for all wheels. On the assumption that left and right tire forces are identical, manipulating Equations (4) and (5) with (9) ~ (11), the longitudinal axle forces can be expressed in terms of the CG location as follows:

$$F_{xf} = -(1 - \chi + a_{x,g} \cdot h / L) \cdot mg \cdot C_x \cdot \frac{V_x - R \cdot \omega_f}{V_x} \tag{12}$$

$$F_{xr} = -(\chi - a_{x,g} \cdot h / L) \cdot mg \cdot C_x \cdot \frac{V_x - R \cdot \omega_r}{V_x} \tag{13}$$

where ω_f, ω_r are the average wheel rotational speeds of left and right wheel, for front and rear, respectively.

The longitudinal axle forces can be determined by rotational dynamics of the wheels as described in Section 2.2. However, Equations (12) and (13) show that two varying unknown parameters, *i.e.* m, C_x, have to be known in order to estimate CG location using longitudinal axle forces.

3.2. Tire Force Ratio Utilization Strategy

The vehicle mass and tire slip slope are not readily measurable and the real-time estimation of these parameters are known as nontrivial task in various actual driving conditions. For this reason, a strategy utilizing a new defined parameter β is proposed, which is defined by the rear-to-front tire longitudinal force ratio. Since the longitudinal axle forces are both proportional to the vehicle mass and the tire slip slope in Equations (12) and (13), it is possible to eliminate these two varying unknown parameters by dividing Equation (13) by (12) as follows:

$$\frac{F_{\mathrm{xr}}}{F_{\mathrm{xf}}} = \frac{\chi - a_{\mathrm{x,g}} \cdot h / L}{1 - \chi + a_{\mathrm{x,g}} \cdot h / L} \cdot \frac{V_{\mathrm{x}} - R \cdot \omega_{\mathrm{r}}}{V_{\mathrm{x}} - R \cdot \omega_{\mathrm{f}}} = \beta \tag{14}$$

Defining the slip ratio of rear to front wheel α and the load transfer factor σ, Equation (14) is expressed as

$$\beta = \frac{\chi - \sigma}{1 - \chi + \sigma} \cdot \alpha \tag{15}$$

where $\alpha = (V_{\mathrm{x}} - R_{\mathrm{ff}} \cdot \omega_{\mathrm{r}})/(V_{\mathrm{x}} - R_{\mathrm{ff}} \cdot \omega_{\mathrm{f}})$ and $\sigma = a_{\mathrm{x,g}} \cdot h/L$.

To obtain precise value of α, vehicle velocity is obtained using GPS because the estimation of vehicle velocity is out of scope of this paper. In addition, the load transfer factor σ can be obtained with the vehicle acceleration sensor. Considering β is determined by rotational dynamics of the wheels, the CG location is the only unknown parameter of Equation (15) and thus can be estimated.

From Equation (15), the basic equation about the longitudinal CG location can be derived as follows:

$$\chi = \frac{(\alpha + \beta) \cdot \sigma + \beta}{\alpha + \beta} \tag{16}$$

In summary, there are three unknown parameters, *i.e.* χ, m and C_{x}, in Equations (12) and (13). Therefore, it is not mathematically possible to obtain the unknowns. However, Equation (16) can give a practical way to remove some unknowns by exploiting the brake force distribution of production vehicles.

3.3. Uncertainty Compensation

The aforementioned basic equation is not capable of providing reliable information about the longitudinal CG location because of uncertainties, including sensor noises and road roughness, that are introduced under real driving conditions. To obtain reliable real-time estimation results, an adaptive law was adopted that reduces the uncertainties.

The normalized CG location χ used for the longitudinal CG location can be estimated based on Equation (16) and an adaptive rule as follows. The normalized CG location χ can be expressed in terms of its nominal value χ_{n} and the deviation χ_Δ as follows:

$$\chi = \chi_{\mathrm{n}} + \chi_\Delta \tag{17}$$

Using Equations (16) and (17), the deviation can be established as

$$\chi_\Delta = \frac{(\alpha + \beta) \cdot \sigma + \beta}{\alpha + \beta} - \chi_{\mathrm{n}} \tag{18}$$

Applying a low pass filter (LPF) to reduce the sensor noise, Equation (18) can be expressed as

$$\dot{z} = -\gamma z + \gamma \chi_\Delta \tag{19}$$

where γ is a positive LPF gain.

Subsequently, the parameter χ_Δ can be estimated using the following equation

$$\dot{\hat{z}} = -\gamma \hat{z} + \gamma \hat{\chi}_\Delta + k(z - \hat{z}) \tag{20}$$

where $\hat{\bullet}$ is an estimated value and k is a positive feedback gain.

In conjunction with this equation, the adaptive law can be written as:

$$\dot{\hat{\chi}}_\Delta = \gamma \varepsilon (z - \hat{z}) \tag{21}$$

where ε is a positive adaptive gain.

Furthermore, the Lyapunov function to analyze the stability of this adaptive scheme can be chosen as

$$V(\tilde{z}, \tilde{\chi}_\Delta) = \frac{1}{2}(\tilde{z}^2 + \frac{\tilde{\chi}_\Delta^2}{\varepsilon}) \tag{22}$$

where $\tilde{z} = z - \hat{z}$ and $\tilde{\chi}_\Delta = \chi_\Delta - \hat{\chi}_\Delta$. The time derivative of Equation (22), after combined with Equation (19), (20) and (21), can be written as

$$\dot{V} = -(\gamma + \varepsilon)\tilde{z}^2 \le 0 \tag{23}$$

Through applying the Barbalat's lemma (Khalil and Grizzle, 1996), it can be concluded that $\tilde{z}$ and $\tilde{\chi}_\Delta$ are converged to zero as time goes to infinity.

4. IDEAL BRAKE FORCE DISTRIBUTION

In respect of the practical use of the proposed algorithm, the estimated CG location was utilized for ideal brake force distribution. The ideal brake distribution is the optimum distribution of front-to-rear braking forces that can prevent premature wheel lock-up from reaching the maximum braking force on all road surface conditions (Limpert, 1999). In most previous vehicle designs, however, the braking forces on the front and rear wheels are designed to have a fixed linear proportion because of the mechanical limits and the lack of the vehicle weight information including CG location (Kim *et al*., 2001). In this paper, the combination of front conventional hydraulic brake and rear EMB that can control the front and rear brake separately is used to realize the ideal brake distribution.

Figure 3 compares the ideal brake force distribution to

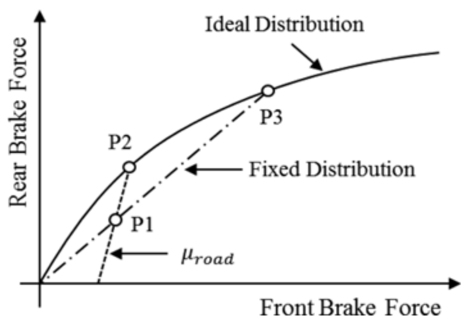

Figure 3. Brake force distribution.

fixed brake force distribution. In case of the fixed distribution, premature front wheel lock-up is generated at the point of P1 when the tire-road friction is lower than the critical deceleration point, P3. On the other hand in case of the ideal distribution, it is possible to reach the maximum point P2 for the given tire-road friction, preventing premature wheel lock-up, so that the total brake force of the vehicle can be maximized. Given the front brake force, the ideal rear brake force can be established by the known equations about ideal brake force (Limpert, 1999) using the estimated CG location as

$$F_{\mathrm{br,ideal}} = F_{\mathrm{bf}} \cdot \frac{\hat{\chi} - a_{\mathrm{x,g}} \cdot h / L}{1 - \hat{\chi} + a_{\mathrm{x,g}} \cdot h / L} \cdot \rho \tag{24}$$

where F_{bf} is the given front brake force and $\rho \leq 1$ is the safety factor which prevents rear wheel lock-up first.

5. SIMULATION RESULTS

The proposed CG location estimation algorithm was evaluated in simulations by implementing it in CarSim, an industry-standard vehicle dynamics simulation software. The normalized CG location of the vehicle model is set by 0.476, but the nominal value is 0.4 for validating uncertainty compensation of the algorithm. The brake force input is determined by the ideal brake force distribution ratio, which is calculated using the estimated CG location while the estimation algorithm is running. The ultimate goal of this simulation studies is to validate the uncertainty compensation of estimation algorithm and to verify the effectiveness of the ideal brake distribution (IBD).

Figure 4 shows the simulation maneuver. The vehicle is decelerated to 1g straightly on the dry asphalt for about 3 seconds. Figure 5 presents the result of the uncertainty compensation of the model. Figure 6 compares IBD using the estimated CG location, IBD using nominal CG location and the fixed brake distribution. The fixed brake distribution

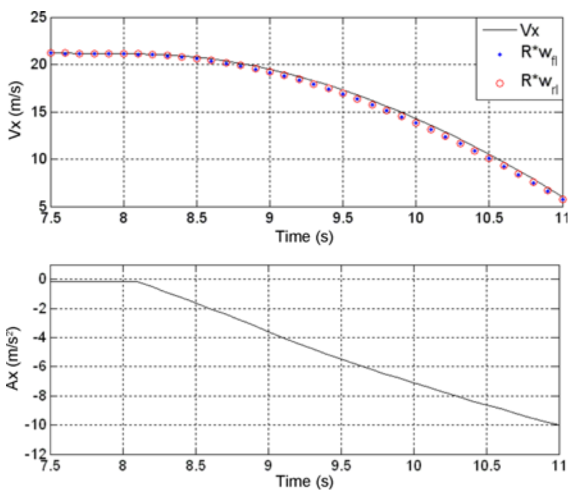

Figure 4. Simulation Maneuver.

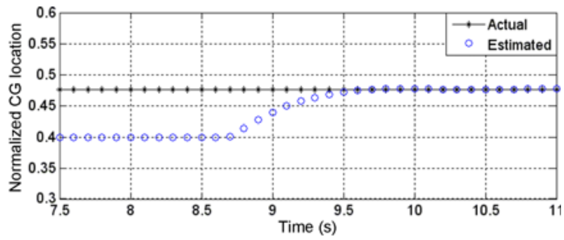

Figure 5. Normalized CG location estimation with uncertainty compensation.

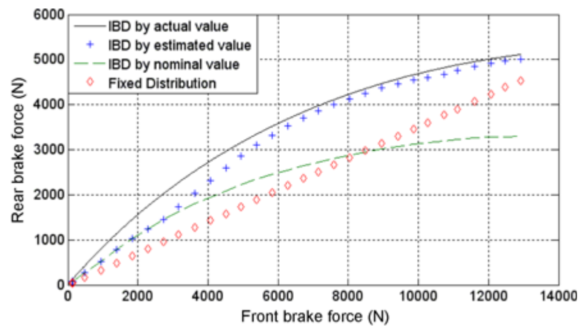

Figure 6. Ideal Brake Distribution (IBD).

ratio, which means the front brake force ratio to total brake force, is set by 0.73 according to the design parameter of the vehicle selected as reference for the simulation. As shown in Figure 5, the uncertainties are effectively compensated by the proposed CG location estimation algorithm and thus the estimated value follows the actual value reliably. Figure 6 shows that IBD using estimated CG location moves much closer to the ideal curve than the fixed distribution as the estimation result approaches the actual one gradually.

On the other hand, IBD using nominal CG location goes under the fixed distribution curve in the deceleration region and this may cause premature front wheel lock in that region.

6. EXPERIMENTAL RESULTS

The experimental evaluation of the developed algorithm

Figure 7. Test vehicle.

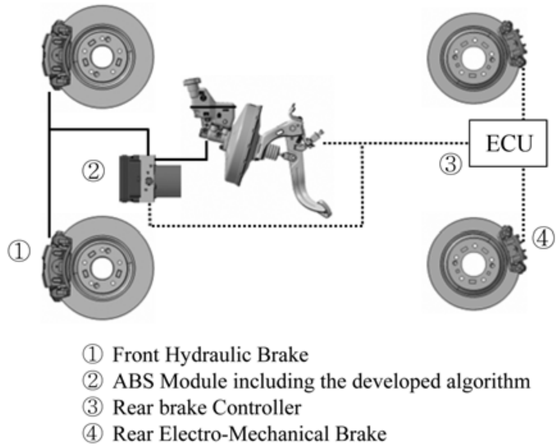

Figure 8. Brake system of the test vehicle.

was conducted on a flat, straight proving ground, using a medium-size production vehicle shown in Figure 7. The longitudinal CG location estimation algorithm was verified under three different weight conditions.

Furthermore, the ideal brake distribution was validated on dry asphalt as well as on wet basalt road to confirm the performance in maximizing deceleration of the vehicle preventing the wheels from locking up under different road conditions.

6.1. Experimental Setup

Figure 8 shows a special brake system which can control the front and rear brake separately to implement the ideal brake force distribution. The EMB were equipped in the rear side of the vehicle whereas the conventional hydraulic front brakes were utilized. The longitudinal velocity of the vehicle is obtained by GPS from VBox of Racelogic. Other variables are obtained from the CAN bus signals or the sensor outputs available from the test vehicle. Main vehicle parameters used in the developed algorithms are L = 2.805 m, R = 0.323 m, $r_{\text{eff,f}}$ = 0.131 m, $r_{\text{eff,r}}$ = 0.124 m, and J_w = 0.7 kgm^2.

6.2. Test Results and Analysis

Three separate experiments were carried out to verify the longitudinal CG location estimation algorithm.

The first experiment was conducted with 65 kg added weight on the front passenger seat. The second and the third experiments were conducted with 160 kg added weight placed on the rear passenger seat and in the trunk, respectively. The mass of the vehicle of the first experiment was 1744 kg and for the other experiments the mass were 1839 kg.

To reinforce the uncertainty compensation for real driving conditions, the final estimation results were calculated by taking a cumulative average of the estimated results acquired by the adaptive law after each braking was completed.

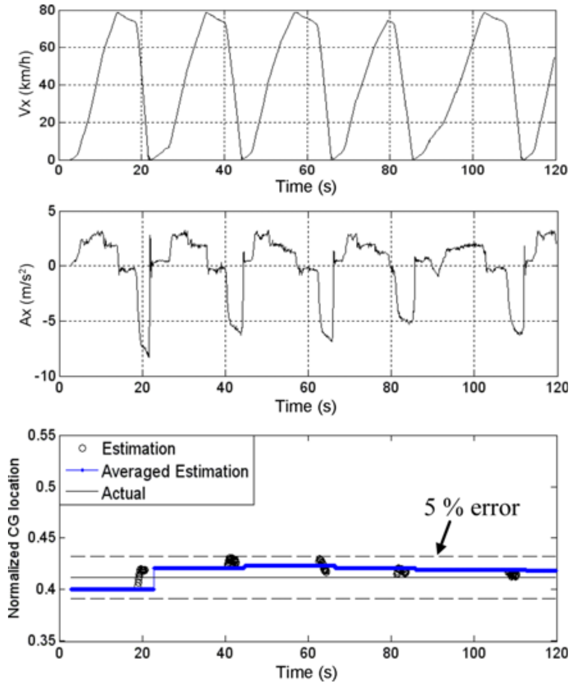

Figure 9. CG location estimation with 65 kg added on the front passenger seat.

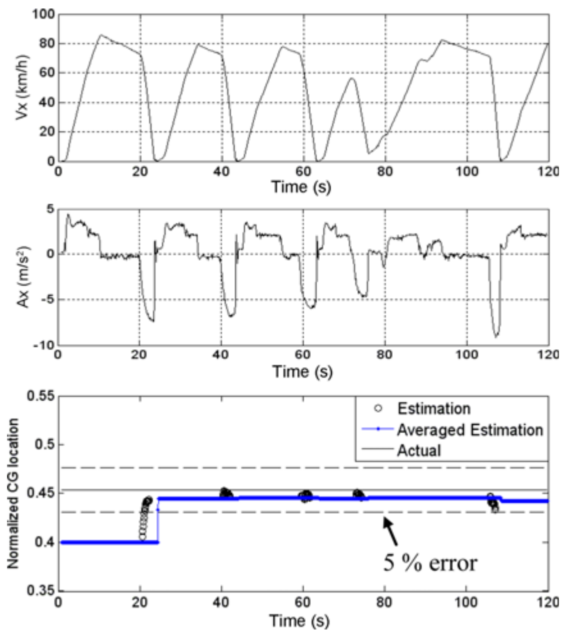

Figure 10. CG location estimation of 160 kg added on rear passenger seat.

Figure 9 shows the results of the first experiment. The vehicle accelerated to 80 kph and then decelerated to 0 kph and similar scenario was repeated several times. The circles on the graph represent the estimation results acquired by the adaptive law. The estimated results lay within the 5 % errors reliably. Figures 10 and 11 present the

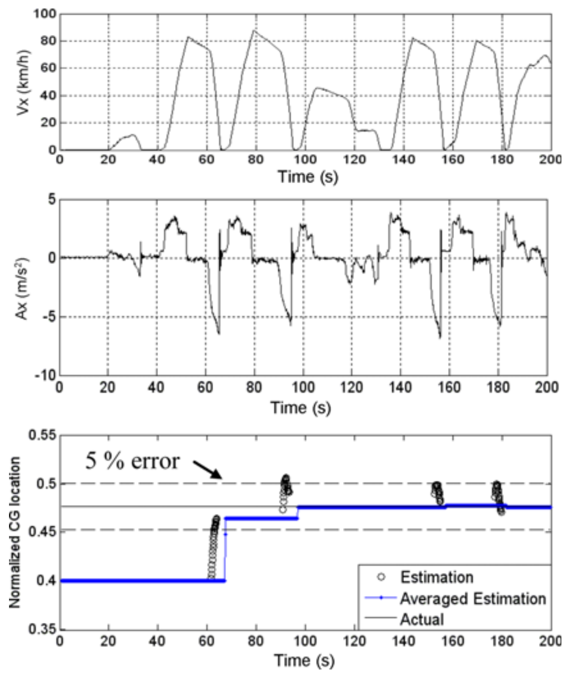

Figure 11. CG location estimation of 160 kg added in trunk.

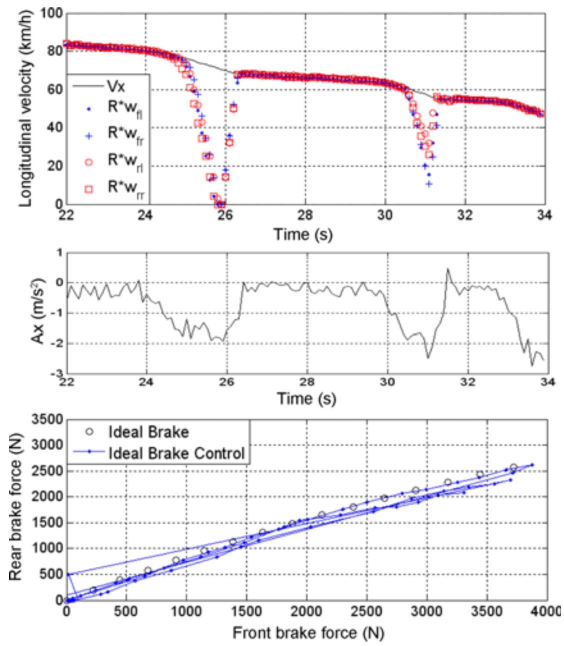

Figure 13. Ideal brake force distribution control on wet basalt road surface with $\mu_{road} \approx 0.2$.

results of the second and the third experiment, respectively. The test maneuvers were conducted in a similar way to that in the first experiment. The results show that the CG location estimation values reach the 5 % error zone quickly during the first braking event and remain in that zone reliably, although the difference between the actual CG location and the nominal value is over 19 % in case of the third experiment. These three experiments show that the developed algorithm can distinguish wide range of CG location changes effectively regardless of the variations in vehicle mass.

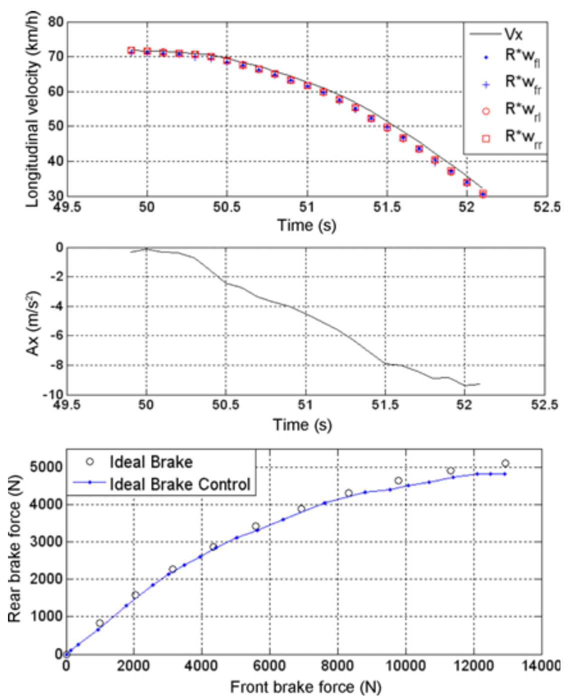

Figure 12. Ideal brake force distribution control on dry asphalt with $\mu_{road} \approx 1.0$.

In addition, the experiments validating the ideal braking distribution were carried out under two different road conditions of the dry asphalt and the wet basalt. These experiments were conducted under the equivalent weight condition of the third experiment of the CG location estimation. The ideal brake force distribution ratio was calculated using the previously estimated value of CG location from the aforementioned third experiment.

Figure 12 shows the results on dry asphalt. The braking was started at 70 kph and the braking force was continuously increased until the vehicle deceleration reaches nearly 1.0 g. The result shows that the braking force was generated in accordance with the ideal distribution. Because of the ideal brake distribution, the vehicle was able to steadily decelerate without generating wheel lock under the severe braking condition.

Figure 13 shows the results on wet basalt road. The braking was started at 80 kph and the braking force was continuously increased until all wheels were locked while ABS control was deactivated to observe the wheel lock behavior effectively. The test result shows that the deceleration was maximized as the four wheels were locked nearly at the same time and that the braking curve follows the ideal braking curve reliably even under the low friction road condition.

7. CONCLUSION

This paper proposed a real-time longitudinal CG location estimation algorithm based on the dynamics of longitudinal braking. To reduce the effects of sensor noises and road roughness, an adaptive scheme was adopted. The contributions of the proposed algorithm include a simple and reliable algorithm for estimating the longitudinal CG location which does not involve the vehicle mass, tire-road friction, vehicle moments of inertia, suspension model information or the tire cornering stiffness. To confirm the practical use of the proposed algorithm, the ideal brake force distribution was tested using the vehicle equipped with the EMB on the rear side. Experimental results demonstrate that the CG location can be estimated fast and quite reliably under various test conditions and that the deceleration can be maximized by the ideal brake force distribution using the estimated CG location. The proposed algorithm in this paper may provide a potentially suitable basis for estimating other parameters, and for application in vehicle safety control systems.

REFERENCES

Choi, S. B. (2008). Practical vehicle rollover avoidance control using energy method. *Vehicle System Dynamics: Int. J. Vehicle Mechanics and Mobility* **46**, **4**, 323−337.

Han, K., Choi, S., Lee, J., Hyun, D. and Lee, J. (2017). Accurate brake torque estimation with adaptive uncertainty compensation using a brake force distribution characteristic. *IEEE Trans. Vehicular Technology* **66**, **12**, 10830−10840.

Huang, X. and Wang, J. (2012). Longitudinal motion based lightweight vehicle payload parameter real-time estimations. *J. Dynamic Systems, Measurement, and Control* **135**, **1**, 011013-1–011013-10.

Huang, X. and Wang, J. (2014). Real-time estimation of center of gravity position for lightweight vehicles using combined AKF-EKF method. *IEEE Trans. Vehicular Technology* **63**, **9**, 4221−4231.

Khalil, H. K. and Grizzle, J. (1996). *Nonlinear Systems*. Vol. 3. Prentice Hall. New Jersey, USA.

Kim, S., Kim, H. and Sung, Y. (2001). Electronic control of braking force distribution for vehicles using a direct adaptive fuzzy controller. *KSME Int. J.* **15**, **1**, 66−80.

Limpert, R. (1999). *Brake Design and Safety*. 2nd edn. SAE International. Warrendale, Pennsylvania, USA.

Pence, B. L., Fathy, H. K. and Stein, J. L. (2014). Recursive estimation for reduced-order state-space models using polynomial chaos theory applied to vehicle mass estimation. *IEEE Trans. Control systems Technology* **22**, **1**, 224−229.

Peng, H. and Hu, J. S. (1996). Traction/Braking force distribution for optimal longitudinal motion during curve following. *Vehicle System Dynamics: Int. J. Vehicle Mechanics and Mobility* **26**, **4**, 301−320.

Rajamani, R. (2006). *Vehicle Dynamics and Control*. 1st edn. Springer. New York, USA.

Rajamani, R., Phanomchoeng, G., Piyabongkarn, D. and Lew, J. Y. (2012). Algorithms for real-time estimation of individual wheel tire-road friction coefficients. *IEEE Trans. Mechatronics* **17**, **6**, 1183−1195.

Solmaz, S., Akar, M., Shorten, R. and Kalkkuhl, J. (2008). Real-time multiplemodel estimation of centre of gravity position in automotive vehicles. *Vehicle System Dynamics: Int. J. Vehicle Mechanics and Mobility* **46**, **9**, 763−788.

Ulsoy, A., Peng, H. and Çakmakci, M. (2012). *Automotive Control Systems*. 1st edn. Cambridge University Press. Cambridge, UK.

Wenzel, T. A., Burnham, K. J., Blundell, M. V. and Williams, R. A. (2006). Dual extended Kalman filter for vehicle state and parameter estimation. *Vehicle System Dynamics: Int. J. Vehicle Mechanics and Mobility* **44**, **2**, 153−171.

Wesemeier, D. and Isermann, R. (2009). Identification of vehicle parameters using stationary driving maneuvers. *Control Engineering Practice* **17**, **12**, 1426−1431.

Yoon, J., Yi, K. and Kim, D. (2006). Rollover index-based rollover mitigation control system. *Int. J. Automotive Technology* **7**, **7**, 821−826.